# Transportation of Water Vapor into the Tibetan Plateau in the Case of a Passing Synoptic-Scale Trough

**Shiori SUGIMOTO, Kenichi UENO**

*Graduate School of Life and Environmental Sciences, University of Tsukuba, Tsukuba, Japan*

**and**

**Weiming SHA**

*Graduate school of Science, Tohoku University, Sendai, Japan*

(*Manuscript received 20 February 2006, in final form 8 September 2008*)

## Abstract

The passing of a synoptic trough is expected to contribute strongly to water vapor (WV) transport processes from the Indian Ocean to the Tibetan Plateau (TP) during the monsoon season. However, the pathway of the WV into the plateau associated with passing a trough and its contribution to the WV budget over the TP are not clear. In this study, the processes of WV transport in the case of a passing trough in 1998 were analyzed using GAME reanalysis data and the numerical model, focusing especially on the WV transportation pattern in the Indian Monsoon region and the diurnal variation of WV intrusion from south of the Himalayas to the TP.

WV advection into the TP was larger in the case of a passing synoptic trough than in the case of a prevailing Tibetan High. Sub-continental scale circulation for the two synoptic types corresponded with active/break phase of the Indian monsoon. In case of prevailing Tibetan High, a cyclonic circulation with a low-pressure area over India, associated with active Indian monsoon phase, prevented the WV intrusion into the TP in the middle troposphere. However, in the case of the trough that corresponded with break phase of Indian Monsoon, WV was transported directly from Arabian Sea to the southern foot of the Himalayas with a northward shift of the low-level monsoon westerly and it intruded into the southeastern TP.

Numerical experiments showed that the WV transport process was composed of multiple steps in the case of the passing trough. WV was transported by the monsoon westerly to the southern foot of the Himalayas at 1500 m above sea level (a.s.l.). The moist air mass reached south of the TP with at about 5500 m a.s.l. during the noon to evening because of the development of a mixing layer and the enhancement of an upslope wind in southern slope of the Himalayas. A moist southwesterly flow was converged latitudinally in the southeastern TP because of the dry northwesterly flow prevailing in the rear of the passing trough over the TP. This convergence area expanded northward from mid-afternoon into the night and disappeared early next morning.

## 1. Introduction

The Tibetan Plateau (TP) is an important heat source for the first transition of the Asian summer monsoon and the maintenance of the monsoon circulation (e.g., Hahn and Manabe 1975; Yanai et al. 1992; Li and Yanai 1996; Ueda and Yasunari

Corresponding author: Shiori Sugimoto, Graduate School of Life and Environmental Sciences, University of Tsukuba, 1-1-1, Tennodai, Tsukuba, Ibaraki, 305-8572, Japan.
E-mail: s0630299@ipe.tsukuba.ac.jp
©2008, Meteorological Society of Japan

1998; Wu and Zhang 1998; Ye and Wu 1998). This heating effect also causes suppression of convection over northern India and formation of arid climate over northeast China associated with making subsidence around the TP (Sato and Kimura 2005, 2007). The release of latent heat associated with active cloud convections over the TP contributes to the direct heating of the middle and upper troposphere (Yanai et al. 1992; Yanai and Li 1994). Atmospheric moisture is an important source of the induction of convective instability and precipitation, which changes the surface wetness and starts land-surface interactions.

Evident diurnal cloud development with weak and frequent precipitation has been observed in the eastern TP during the monsoon season (e.g., Ueno et al. 2001; Uyeda et al. 2001), although the absolute amount of atmospheric moisture is small compared to that at lower elevations because of low-pressure and low-temperature conditions. The active water cycle is maintained by land-atmosphere interactions with a certain amount of water vapor (WV) supply coming into the column of the atmosphere over the TP. The WV supply follows two routes: evaporation from land-surface and advection from outside the TP. Using numerical simulations, Numaguti (1999) estimated that the contribution of WV evaporating from the northern Indian Ocean to the precipitating water over the TP was more than 50% of all oceanic origins. They also indicated that the recycling rate of precipitation between the atmosphere and the land surface was about 35% over the TP. Based on stable isotope observations, Tian et al. (2001) indicated that oceanic-originated moisture, perhaps evaporated from the Bay of Bengal (BoB), was the main source of WV in the southern TP. These results indicate that the WV advection from outside the TP strongly contribute to the water cycle activity over the TP, and the timing and mechanisms of WV intrusion in conjunction with intraseasonal variability of Indian monsoon need to be revealed.

Synoptic condition around the TP during monsoon season changes under the influence of variability of mid-latitude westerly. Yamada and Uyeda (2006) focused on the differences in synoptic conditions, such as the prevailing cumulus convection with a dominant Tibetan High (Upper High; UH type) and the passage of a synoptic disturbance (TROUGH; TR type), and they detected that a cumulus structure of the UH type changes with the moistening of the land-surface. Mid-latitude oscillation effects on this intraseasonal variability of precipitation activity over the TP. Fujinami and Yasunari (2001, 2004) stated that the timescale of intraseasonal variability in convective activity over the TP was about 14 days and was composed of an east-west oscillation of the Tibetan High in the upper troposphere and the southward extension of the mid-troposphere trough. For the WV transport process from outside the TP, passing a trough is expected to be an important function. For example, Ueno (1998) analyzed evident moisture intrusion from south of the TP at a 500-hPa level for westward movement of a synoptic trough with meandering westerlies, which caused the first heavy precipitation of 1993 monsoon. According to stable isotope observations in August 2004, WV originated from remote areas, not from a local source, contributes to occurring precipitation with a passing trough case (Kurita and Yamada 2008). Yasunari and Miwa (2006) pointed out that plateau edge cyclogenesis occurred with the enhancement of a southerly moisture inflow from the Indian plain in association with movement of large-scale westerly troughs onto the TP and caused heavy rain in the Yangtze River basin. These results suggest that the synoptic-scale trough plays an important role in the intrusion of moist air advection into the plateau. WV trajectory in large-scale is supposed to be controlled by the linkage between the activity of synoptic-scale trough and the Indian monsoon.

It is well known that the Indian monsoon has an active/break phase with a timescale of about 15 days or 30–50 days and that the precipitation amount increases or decreases over central India in the active or break phase, respectively, of the Indian Monsoon (e.g., Murakami 1976; Kurishunamurti and Bhalme 1976; Yasunari 1979; Yasunari 1980; Yasunari 1981; Pant 1983). The timescale of about 15 days is explained by north-south oscillation of monsoon westerlies (Murakami 1976, 1977). The 40-day timescale is caused by the northward movement of cloud disturbance over the Asian monsoon region (60°–120°E), which is initiated by eastward propagating of clouds corresponded with the Madden-Julian Oscillation (e.g., Yasunari 1979; Yasunari 1981; Lau and Chan 1986). Chang (1981) indicated an inverse correlation between the precipitation amount in central India and that in the central TP with the timescale of about 15 and 40 days. In other words, the active phase of the Indian monsoon corresponded to the break phase of the plateau monsoon, meaning that active WV supply

into the TP could occur during the break phase of the Indian monsoon. Effects on phase changing of Indian monsoon to the sub-continental scale WV pathway to intrude into the TP needs to be discussed in this paper.

One important factor affecting WV transportation into the TP is the function of the Himalayas, which usually prevent the dynamic intrusion of WV into higher elevations. Local circulation with a strong daytime wind speed has been observed along deep valleys in the Himalayas (Ohata et al. 1981; Bollasina et al. 2002; Ueno et al. 2008). Inoue (1976) observed an increase in relative humidity with daytime valley winds. A weak southerly wind continues during the night in the monsoon season, which accompanies nocturnal precipitation at the foot and in the valley of the Himalayas (Barros et al. 2000; Ohsawa et al. 2001; Ueno et al. 2001b; Bollasina et al. 2002). Barros and Lang (2003) proposed a mechanism of nocturnal precipitation by a weakening of the nighttime valley wind, stagnating the WV in front of the Himalayas. Sasaki et al. (2003) conducted numerical experiments to reveal the WV transport process over the south of TP during the post-monsoon season (October in 2000), and they showed that WV penetrated some cols of the Himalayas associated with a diurnal variation caused by a heating contrast between the TP and the Hindustan plain. At the same time, local circulation functioned to redistribute the precipitable water between the mountain and valley when there were weak general flows over the TP (Takagi et al. 2000; Kuwagata et al. 2001). Kurosaki and Kimura (2002) revealed using the satellite images that afternoon high-level clouds distributed according to the major topography were caused by thermally induced local circulation. However, the contribution of such topography-influenced local circulation to diurnal changes of WV distribution in a prevailing trough system has not been examined. Numerical experiments dealing with the diurnal development of moist convection are useful for determining the effect of topography on the WV transport process over complex mountain ranges south of the TP.

The aim of this study is to reveal when and how WV is transported to the TP with a prevailing synoptic-scale trough. First, the difference of WV advections over the TP between the two different synoptic conditions (TR and UH type) was clarified using reanalysis data. Second, the flow pattern of WV south of and over the TP was identified, and the relation between the intraseasonal variability of the synoptic condition and the transport pathway was clarified. Finally, we carried out numerical simulations to understand temporal changes in WV transport around the Himalayas and over the TP in a typical case of the passing of a synoptic trough.

## 2. Analysis methods, data, and model

### *2.1 Analysis methods and data*

First, the general WV flow around the Indian subcontinent was examined using reanalysis data. Recently, we can use various reanalysis data, such as ERA40 (Uppala et al. 2005), JRA25 (Onogi et al. 2007), and the GAME reanalysis which produced after intensive observations in the Asian monsoon region as a part of the GAWEX Asian Monsoon Experiment (GAME) project (Yasunari 1988). The GAME reanalysis data were generated by assimilating the observed data, including more than 100 sonde sites and wind profiler sites (Yamazaki et al. 2003). The horizontal resolution of topography using assimilation was 0.5625 degrees, and the highest horizontal resolution of released data was 0.5 degrees in the Asian monsoon region. On the other hand, in ERA40 and JRA 25 with 2.5- or 1.25-degree grid spacing in a global region, not only radiosonde data but also satellite radiance and wind data were assimilated. Observation data of the GAME project were also included in JRA 25. Differences in subcontinental scale circulations around the TP based on ERA40, JRA25, and the GAME reanalysis were examined to verify a candidate of reanalysis data to use in this study. The depth of the monsoon trough over northern India, the pathway of the monsoon westerly, and the intensity of the synoptic trough in the middle troposphere for TR type, the structures of which are described in detail in Section 3.1, were similar in the three data sets. The wind speed of the low-level monsoon westerly over the Arabian Sea and the southwesterly flow in front of a synoptic trough at 500 hPa in ERA 40 was about 2 m $s^{-1}$ smaller in the ERA40 than in the JRA25 or GAME reanalysis. According to JRA25 data, the specific humidity in northern India was about 3g/kg higher than that shown by other analysis data. However, those differences do not affect for investigations of the WV transport pathways with different synoptic-scale patterns. Therefore, GAME reanalysis with a 0.5-degree grid interval and higher resolution was used in this study because it was useful for obtaining initial and boundary data of a fine-mesh numerical simulation. The mature monsoon season (from July to August)

of 1998 was chosen for the analysis period, when the GAME project achieved intensive sonde data to enhance the GAME reanalysis. Fujinami and Yasunari (2004) revealed that this period also corresponded to prominent intraseasonal variability over the TP.

To investigate large-scale circulation focusing on the differences between the UH and TR type, dominant cases were selected on the GAME reanalysis field. The TR type was specified according to two criteria: 1) the geopotential height at 500 hPa, averaged over an area of 30–40°N and 85–95°E, decreased more than 20 m with a minimum height of less than 5860 m, and 2) a trough was recognized over the TP in the 500 hPa synoptic chart. The UH type stipulated that the 200 hPa geopotential height averaged over an area of 30–40°N and 85–95°E reached more than 12615 m for three consecutive days. Accordingly, five or four cases which included a total of 10 or 16 days were chosen for TR or UH types, respectively (Table 1). Almost all of the selected cases were the same as the UH and TR, as classified by Yamada and Uyeda (2006).

Next, the WV transport process in a TR type affected by complex terrain, including the Himalayas, was diagnosed by using a numerical experiment. METEOSAT-5 infrared (IR) images obtained from EUMETSAT were used to validate the simulated results. Details of the numerical model are given in the next section.

### 2.2 Numerical experiments

Analysis areas (Fig. 1) consist of undulating landscapes, including the Hindustan Plain, the Great Himalayas, the Yarlung Zangbo basin and the Nyainqentanglha mountain range. The Himalayas have a super-complex topography, with more than a 3000 m gap in altitude and a valley width of about 1 to 10 km. The local circulations over the complex terrain were not captured in the 0.5 degree grid of the reanalysis data. We conducted a numerical simulation by a three-dimensional model which simulated the precipitation process under a non-hydrostatic condition and increased the temporal and spatial resolution from 0.5 degree to less than 10-km grid spacing by nesting. From this numerical experiment, the WV transport process with temporal variations from the foot of the Himalayas to the TP was identified.

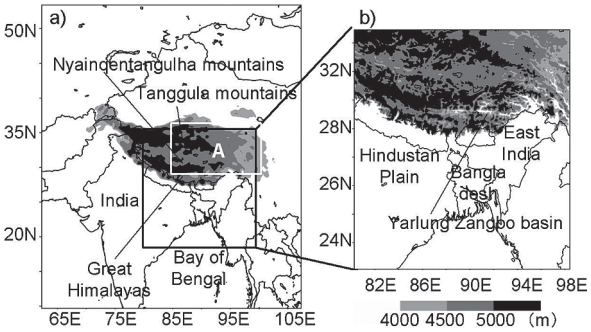


Fig. 1. a) First domain and b) second domain of the NHM simulation over 4000 m a.s.l. (shaded). White box (A) indicates the analysis area of WV advection, as explained in Section 3.1.

A non-hydrostatic model developed by the Meteorological Research Institute and the Numerical Prediction Division of the Japan Meteorological Agency (MRI/NPD-NHM; NHM hereafter) was used in this study. The numerical experimental conditions are shown in Table 2. The fundamental equations are three-dimensional, non-hydrostatic and full compressional. The bulk method including the cold rain process was chosen for cloud microphysics (Ikawa and Saito 1991). In this method, the water substance is classified into six components (water vapor, cloud water, cloud ice, rain, snow, and graupel), and the mixing ratio of each component is calculated. The transformation process of water, including graupel, is important for simulating the precipitation process because, as indicated

Table 1. Analysis periods for the cases of the TR and UH types during the 1998 monsoon.

| | TR type | UH type |
|---|---|---|
| Case 1 | 18 UTC, July 6 – 18 UTC, July 8 | 18 UTC, July 1 – 18 UTC, July 4 |
| Case 2 | 18 UTC, July 23 – 18 UTC, July 25 | 18 UTC, July 17 – 18 UTC, July 19 |
| Case 3 | 18 UTC, August 2 – 18 UTC, August 4 | 18 UTC, July 26 – 18 UTC, August 2 |
| Case 4 | 18 UTC, August 11 – 18 UTC, August 13 | 18 UTC, August 5 – 18 UTC, August 9 |
| Case 5 | 18 UTC, August 16 – 18 UTC, August 18 | |

Table 2. Computational scheme

| | |
|---|---|
| Fundamental equation | Three-dimensional, non-hydrostatic and full compresive |
| Handling of sound wave | Horizontal: explicit,<br>Vertical: HE-VI (Ikawa, 1988; Ikawa and Saito, 1991) |
| Vertical coordinate | Z*-coordinate |
| Cloud microphysics | Bulk method include cold rain (Ikawa and Saito, 1991) |
| Convective parameterization | Kain-Fritsch scheme (Kain and Fritsch, 1990) |
| Horizontal grid-spacing | 30 km and 6 km |
| Vertical grid-spacing | Unequal (40–1200 m) |
| Vertical layers | 38 layers |
| Initial and boundary condition | GAME-reanalysis data (ver. 1.5, 0.5° grid-spacing) |

by Uyeda et al. (2001), the formation of graupel particles is a characteristics of convective clouds over the southeastern TP. The Kain and Fritsch scheme (Kain and Fritsch 1990), which is suitable for calculating cumulus convection at middle latitudes, was used. The evapotranspiration efficiency and albedo are 0.3 and 0.2 for land and 1.0 and 0.6 for ocean grids, respectively. The GAME reanalysis data with a grid spacing of 0.5 were used for the initial and boundary conditions. The calculation was started 12 to 24 hours prior to each analysis period for spinup (Table 3). The vertical coordinate was the Z*-coordinate with an unequal grid interval. The minimum layer depth was 40 m at the lower layer, and the maximum layer depth was 1200 m in the upper layers. The horizontal resolutions for a coarse domain and a nesting domain were 30 km and 6 km, respectively. The 30-km grid spacing was nested in the GAME reanalysis data every 6 hours, followed by 6-km grid spacing nested in the 30 km simulation every 3 hours by a one-way nesting scheme. An interpolated topography data set in each grid size extracted from GTOPO30, which obtained from United States Geological Survey, was used in the model. Topographic features of the numerical domains are shown in Fig. 1. In the first domain, with 30-km grid spacing, the Tanggula and Nyainqentanglha mountains are recognized (Fig. 1a). The complex topographic features in the TP and major valleys transecting the Himalayas can be recognized only in the second domain, with 6-km grid spacing (Fig. 1b). Both domains were set as large as possible for computational efficiency.

Table 3. Periods of NHM simulation for the TR type.

| | Calculated periods |
|---|---|
| Case 1 | 18 UTC, July 3 – 06 UTC, July 10 |
| Case 2 | 06 UTC, July 23 – 06 UTC, July 27 |
| Case 3 | 18 UTC, August 1 – 06 UTC, August 6 |
| Case 4 | 18 UTC, August 10 – 06 UTC, August 15 |
| Case 5 | 18 UTC, August 15 – 06 UTC, August 20 |

## 3. Results

### *3.1 Variation of intraseasonal circulation and water vapor pathway*

WV transportation from the Indian Ocean to the plateau is expected to be affected by sub-continental scale changes in Indian monsoon flows. In this section, a relation between the WV transport pathway in south-east Asia, including the TP, and the intraseasonal variability of the Indian monsoon was revealed. First, horizontal WV advection was calculated for UH and TR types in the domain of 28–35.5°N, 85–100°E (A in Fig. 1) and compared with the WV advection from different directions (Fig. 2). The WV inflow from each direction was integrated between 500 and 300 hPa in the GAME reanalysis data. A daily average WV budget of $1.9 \times 10^{12}$ kg day$^{-1}$ converged in the case of the TR type. Mean-

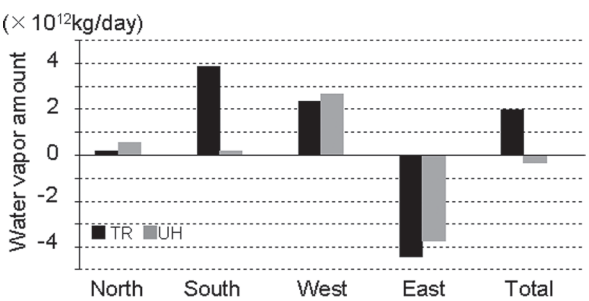


Fig. 2. WV budget calculated in Box A (see Fig. 1), in the cases of the TR (black) and UH (gray) types. Positive/negative values correspond to the inflow/outflow of WV flux.

while, the convergence amount for the UH type was nearly 0 kg day$^{-1}$, meaning that a large amount of WV intrusion from outside occurred for the TR type. For both types, about $2.5 \times 10^{12}$ kg of WV per day came in from the western boarder while about $4 \times 10^{12}$ kg WV went out to the eastern boarder, including that there was little convergence of WV along the east-west direction over the TP. On the other hand, the southerly advection was larger for the TR type and accounted for about 60% of the total inflow from all directions. The combined evidence indicates that the intrusion of WV into the TP from the south dominated for the TR type but not the UH type.

Next, in order to identify the main pathway of WV transport over the south of the TP, WV flux and geopotential height at the lower (850 hPa) and middle (500 hPa) troposphere were compared for the two types (Fig. 3). At 850 hPa (upper two figures in Fig. 3), the distributions of geopotential height differed over the Indian subcontinent. In the case of the UH type, a monsoon trough expanded southward over north India ($\alpha$ in Fig. 3a), and a large latitudinal pressure gradient occurred over southern India with an intensification of the monsoon westerlies (shown as larger vectors in Fig. 3b). The route of westerlies changed towards the north with cyclonic rotation over the northern BoB. Part of this northerly flow intruded westward along the monsoon trough extending in front of the Himalayas. In contrast, the low-pressure zone over the northwest of India ($\alpha$) shrank in the case of the TR type (Fig. 3e), with a shift in the flow axis north toward the foot of the Himalayas (Fig. 3f). Accordingly, the main monsoon westerly channel passed over the central Indian subcontinent from the Arabian Sea to reach the Himalayan ranges directly. The pathway of the TR type obviously differed from the low-level flow patterns generally recognized in the monsoon season (e.g., Kesshavamurty and Awade 1970; Fujinami and Yasunari 2004) that indicating prevailing southeasterly flows from the BoB to the TP, as shown in Fig. 3b. In other words, the UH type flows represent the features of averaged Indian monsoon flows. Murakami (1976) revealed an intraseasonal oscillation of the Indian monsoon on a 15-day time scale that accompanied the north (south) shift of monsoon westerly in the break (active) phase. Precipitation in northern India increases during the break phase of the monsoon in central India (i.e., Kurishnamurthy and Shukla 2000; Goswami and Mohan 2001). Murakami (1986) also pointed out that the precipitation amount at the foot of the Himalayas had an inverse correlation with the precipitation amount in central India because of a change in the WV pathway with the oscillation of monsoon westerlies. The daily average precipitation amount, analyzed using Global Precipitation Climatology Project (GPCP) data, over the southern foot of Himalayas in the present case of the TR type was larger than in the case of the UH type (figures are omitted). Accordingly, the differences between the UH and TR types in terms of the sub-continental-scale flow patterns with latitudinal shifting of the major WV transportation paths under synoptic-scale conditions correspond to the changing phases of the Indian monsoon.

The vertical distributions of specific humidity and flux along the main westerlies in the case of the UH and TR types (transect A-B-C and D-E-F in Fig. 3) are compared in Fig. 4. The distribution of specific humidity showed a similar structure in both types. For example, there was a decrease in WV with an increase in height (Figs. 4a and c), and the main flow of WV was below 700 hPa (Figs. 4b and d). However, the flux near the southern slope of the Himalayas differed between the two types. The amount of WV intrusion over the TP was larger in the case of the TR, corresponding to Fig. 2. A larger WV flux appeared from Bangladesh toward the southeastern TP at 500 hPa in the case of the TR type. This difference was also recognized in the flux distribution of 500 hPa (Figs. 3d and h). In the geopotential height fields of the mid-troposphere for the UH type (Fig. 3c), a low-pressure area existed with its center at 18°N, 80°E. A cyclonic flow associated with this low-pressure area played an important function in changing the WV from the BoB westward before reaching to the TP. It moved to the Arabian Sea, passing over northern India (Fig. 3d). Mujumdar et al. (2005) identified a similar cyclonic circulation over India in the middle troposphere during the active phase of the Indian monsoon. Therefore, the appearance of a low-pressure area in the case of the UH type is quite reasonable in the active monsoon phase in India. The formation mechanism of the low pressure is the southward tilting of a low-level monsoon trough with an increase in altitude (Rao and Ramamurthy 1968) or a cut-off low after passing a trough at 500 hPa by the dynamic effect of TP (Yanai and Wu 2006). In the case of TR type, the low-pressure area disappeared over India at 500 hPa (Fig. 3g), and weak westerlies prevailed there (Fig. 3h). A strong

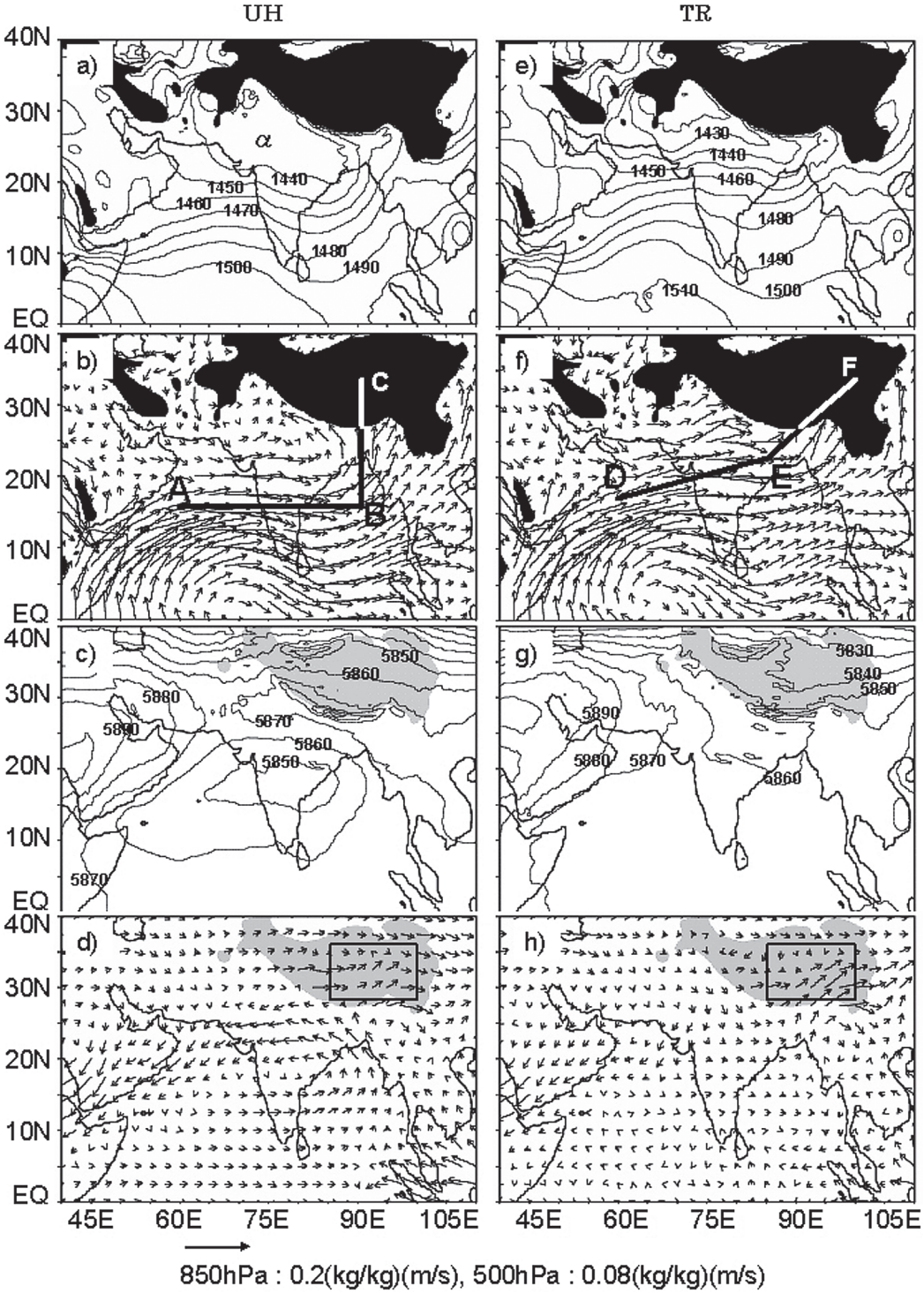


Fig. 3. Composites of geopotential height (unit; m) and WV flux (unit; kg/kg × m $s^{-1}$) at 850 hPa (upper four figures), as well as 500 hPa (lower four figures). Left (right) figures correspond to the UH (TR) type. Areas above 1500 m are masked out with black shading at 850 hPa, and areas higher than 3000 m are shaded light gray at 500 hPa. Open boxes in d) and h) correspond to Box A in Fig. 1. $\alpha$ in a) means monsoon trough. A vertical cross-section of specific humidity and WV flux along the transections A-B-C and D-E-F is shown in Fig. 4.

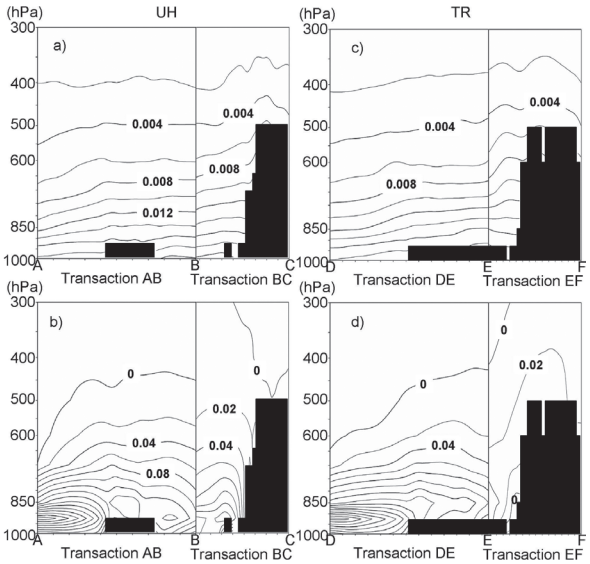


Fig. 4. Height cross-sections of specific humidity (upper) and WV flux (bottom) in the case of the UH type (left) and TR type (right). The cross-sections for the UH type is along the transection A-B-C in Fig. 3b, and that for the TR type is along D-E-F (right) in Fig. 3f. The contour interval of specific humidity (kg/kg) is 0.002, and that of WV flux (kg/kg × m $s^{-1}$) is 0.02. Topography is shaded black.

southwesterly flux corresponding to the front of synoptic trough expanding around 25–32°N, 90–100°E also appeared over Bangladesh (Fig. 3g).

Consequently, differences between the UH and TR type in terms of the large scale circulation in the south of the TP corresponded with the active/break phase of the Indian monsoon and changed the WV flux direction at the mid-troposphere near the southern periphery of the TP through the establishment of cyclonic circulation with a low-pressure system over the Indian subcontinent, which affected the moisture budget over the southeastern TP. Results of objective-analysis data are inconclusive regarding the moisture transportation near the massive topographical features, such as the Himalayas. Mountain ranges usually induce local diurnal circulation, which plays an important role in low-level moisture transportation that is unrecognizable in the reanalysis data. In the next section, details of the WV transport process were again identified for the TR type through the use of a non-hydrostatic numerical model around the southeastern TP.

### *3.2 Transport process of water vapor intruding into the southeastern TP*

To consider the WV transport process into the TP, we need to reveal the mechanisms of WV to crossing over the Himalayas, which usually act as a barrier to atmospheric flow. A high resolution numerical simulation by the NHM was performed for five cases of the TR type (Table 3). In this section, the WV transport process from the lower elevations south of the Himalayas to 4000 m level over the southern TP was detailed for Case 1, when the deepest and largest trough expanded over the southern TP. Hereafter, NHM simulations are described as NHM_30 and NHM_6, with grid sizes of 30 and 6 km in different domains (see Fig. 1), respectively.

First, the reproducibility of synoptic and plateau-scale circulations by the NHM was validated by GAME reanalysis and METEOSAT5-IR data. For all cases listed in Table 3, a westerly wind accompanied by a low-level monsoon westerly over northern India and a Tibetan High centered over the western TP in the upper troposphere were simulated well in NHM_30 (figure was omitted). In Figs. 5a and b, the GAME reanalysis and NHM_30 for 7–8 July showing geopotential height and wind vectors at 500 hPa are compared. The geopotential height distribution showed two troughs separated north-to-south around 90°E and controlled WV intrusion in the southern TP all day on 7–8 July. One of the troughs is in the north of the TP (around 45°N, 95°E; TR1), and the other is over the TP (around 30–35°N, 80–98°E; TR2). A westerly flow penetrates the two troughs along 35–40°N. Large-scale circulation patterns over the TP, represented in the GAME reanalysis, were also simulated by the NHM.

On the other hand, in the case of the NHM_30, a mesoscale cyclonic circulation (Low_A) was formed at the center of the TP at 06 LT on 7 July. This Low_A migrated northeastward and reached 35°N, 100°E at 18 LT on 8 July. Westerlies along 35–40°N converged with easterlies in the northern part of TR2 (Line_B). A similar circulation and low-pressure system with a convergence line were recognized in four other TR cases by the NHM simulations. Cloud areas in the METEOSAT-5 IR images (Fig. 5c) were compared with the results of NHM_30 in order to examine in detail the formation of disturbances. Over the southern

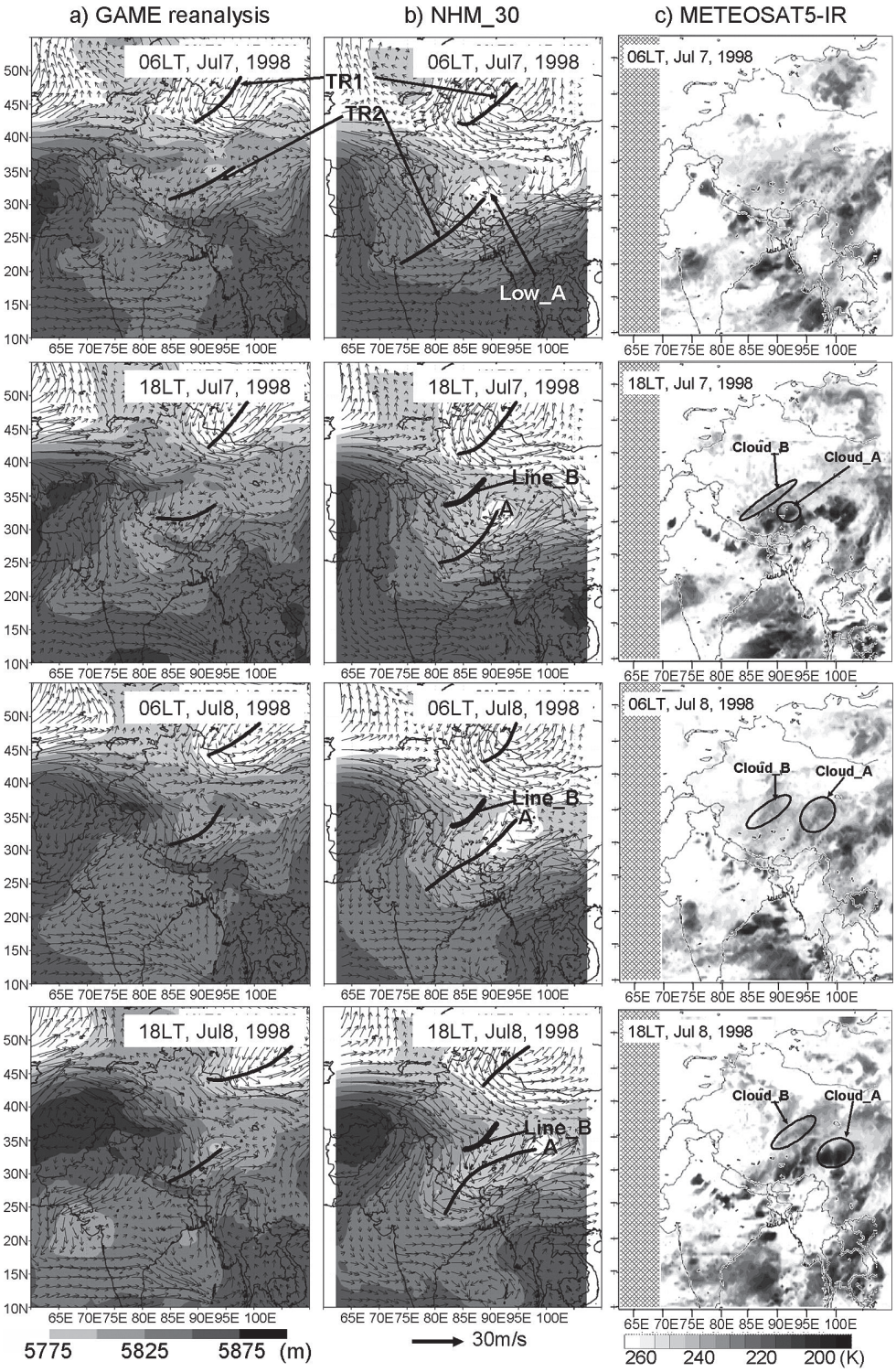


Fig. 5. Geopotential height and wind vector at 500 hPa for a) GAME reanalysis data, b) NHM_30, and c) the METEOSAT-5 IR images at 06 and 18 LT on 7–8 July. TR1and TR2 indicate two troughs. Low_A (or A) indicates a mesoscale cyclonic circulation over the TP. Line_B indicates a convergence line. Cloud_A and Cloud_B indicate convective zones accompanied by Low_A and Line_B. These marks are explained in Section 3.2.

and southeastern TP, a cloud area corresponding to TR2 was discernable from the afternoon into the night. Cloud convections were very active ahead of TR2, with southwesterlies crossing over the eastern Himalayas. In addition, a mesoscale convection (Cloud_A) developed in the same area of the Low_A in NHM_30. Over the western TP, a dry intrusion with cloud-free areas distributed with the forming cloud zone (Cloud_B) at a head, which was consistent with the formation of Line_B by NHM_30. This evidence confirmed that the NHM could simulate the mesoscale circulation and the convergence zones over the TP.

Temporal changes of WV distribution around the Himalayas were identified by fine-mesh simulation results (NHM_6) nested in the NHM_30. Figure 6 shows wind and specific humidity at three-hour intervals at 1500 m a.s.l. on two successive days (7–8 July). Moist air was flowing from the west along the foot of the Himalayas about 2000 m a.s.l. below on 7 July. This flow was a part of the main monsoon westerly intruding from the Arabian Sea (shown in Fig. 3f). In the afternoon, specific humidity increased in wider areas, especially over Bangladesh and East India. The simulated potential temperature profile showed that the mixing layer depth over the south of the Himalayas was around 500 m in the early morning but developed to 1500 m in the afternoon (figures are omitted). Therefore, the increase in moisture could be explained by two factors: the low-level intrusion of moist air associated with monsoon westerlies and the development of a mixing layer over the land.

During the afternoon, the wind direction also changed from west to southwest over Bangladesh. As shown by latitude-height sections of wind speed along 93°E (left in Fig. 7), an upslope wind was simulated all day but was enhanced in the mid-afternoon in the southern slope of the Himalayas. This diurnal change of wind speed in the Himalayan slope was consistent with the findings of past observational studies (Ohata et al. 1981; Bollasina et al. 2002; Ueno et al. 2008). WV flux from the south of the Himalayas increased along with the enhancement of daytime wind speed (Fig. 7, right). The afternoon increase in WV flux corresponded to the findings of a past observation (Inoue 1976). Therefore, the simulation by NHM_6 suggested that a strong daytime upslope wind near the Himalayas transported WV in the mixing layer from low elevations to high elevations over the southern TP. From midnight to the next morning, the specific humidity in the lower elevations decreased due to the disappearance of the mixing layer. A similar diurnal variation of WV distribution was repeated on 8 July. Accordingly, in the NHM simulation, WV transportation in front of the Himalayas was controlled by several important systems, such as a low-level rich moisture intrusion from the west, the daytime development of a mixing layer, and a strong upslope wind intruding into the TP.

Finally, characteristics of the WV distribution over the southern TP were analyzed after the intrusion. Figure 8 shows the flux and specific humidity at 5500 m a.s.l. on 7–8 July. Areas above 5000 m a.s.l are shaded light gray. A wetter zone of more than 0.008 kg/kg (shaded dark) appeared south of 29°N at 12 LT. This zone was formed with a convergence between a wetter southwesterly wind intruding from the south of the TP and drier northwesterly winds in the rear of the trough and was consistent with an active convective zone ahead of TR2, as shown in Fig. 5. The moisture zone expanded northeastward by the evening intensification of the southwesterly crossing over the Nyainqentanglha mountains (about 31°N). The wetter zone disappeared from midnight to early next morning due to the weakening of a moist southwesterly crossing over the Himalayas. A similar moisture convergence was repeated on 8 July. Using results of a numerical experiment of WV transport in October, Sasaki et al. (2003) indicated that southerly upslope winds with a moist air mass in a valley of the Himalayas intruded into the southern TP, and general westerlies over the TP formed a stationary moisture front. Although they showed only the contribution of an upslope wind for WV intrusion, our simulation results suggest that the circulation pattern associated with the synoptic trough affected the distribution of WV over the southeastern TP. Namely, WV transported from the southern foot of the Himalayas converged zonally over the southern/southeastern TP but did not expand widely into the central TP due to northwesterlies following the trough from the afternoon into the night. The effect on the WV convergence of a diurnal-induced upslope wind along the southern slope of the Himalayas and the synoptic flow pattern over the TP were systematically driven in the case of the TR type, and this WV transport process was different from the WV redistribution caused by the local circulation with mountain ranges, as explained by Takagi et al. (2000) and Kuwagata et al. (2001).

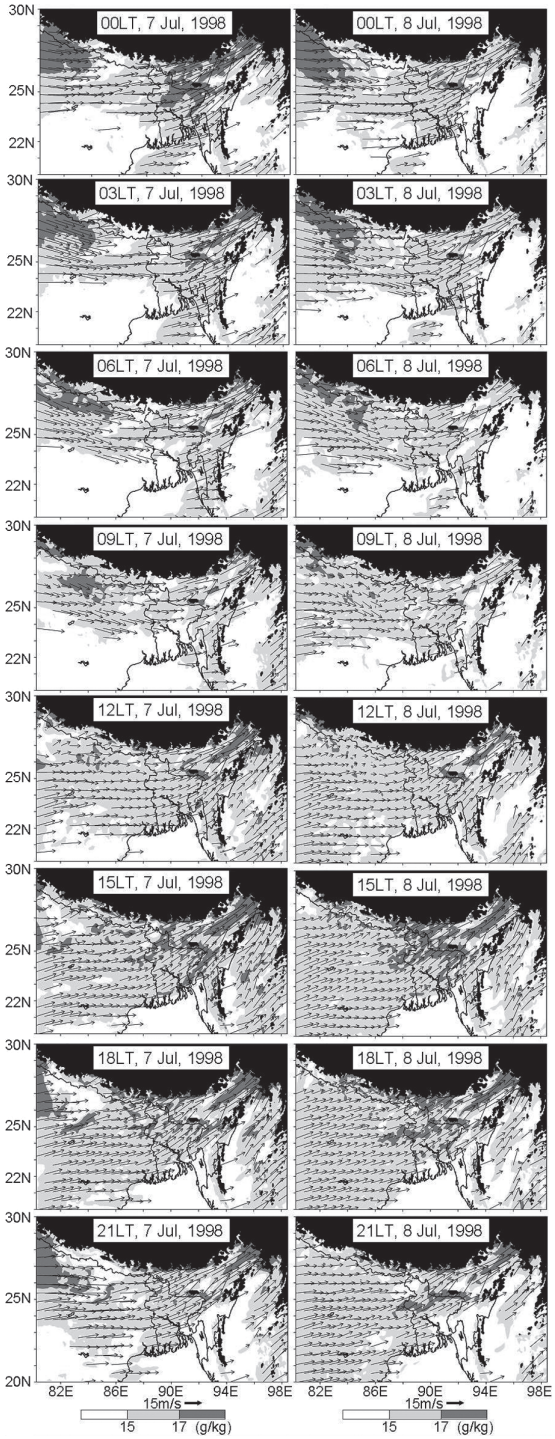


Fig. 6. Wind and specific humidity changes at 1500 m a.s.l. for 7–8 July. Wind vectors are shown only in the shaded area. Specific humidity follows the color legends given at the bottom of the figures. Areas higher than 1500 m a.s.l. are shaded in black.

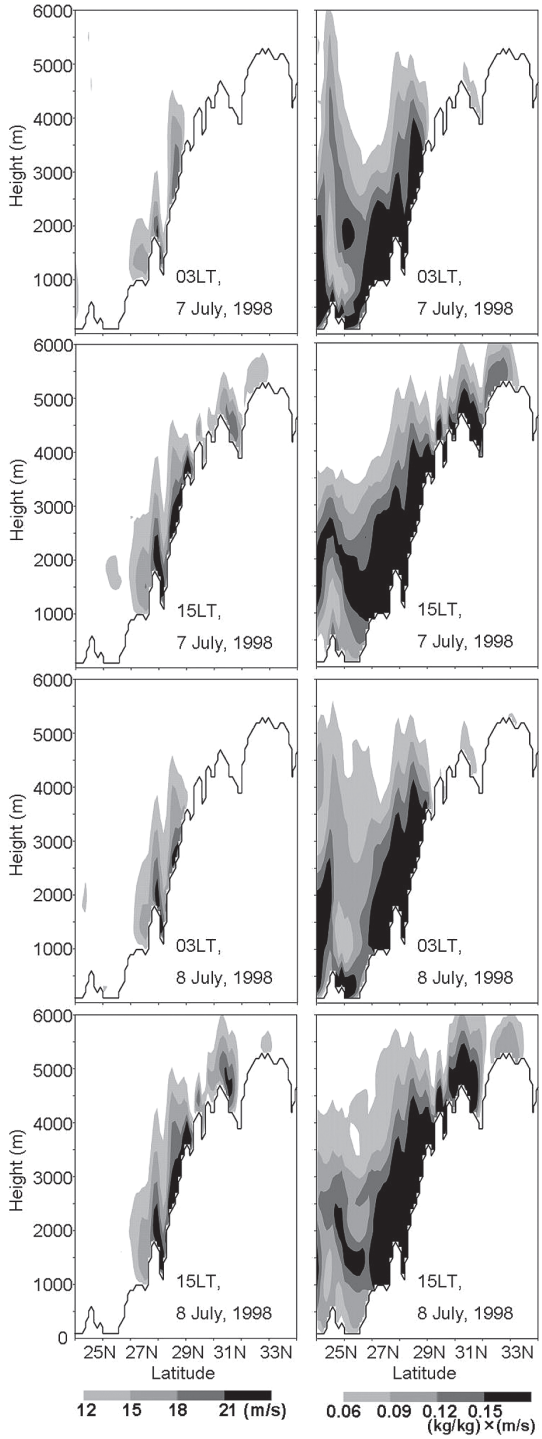


Fig. 7. Latitude – height cross-sections of wind speed (left) and the v component of WV flux (right) along 93°E in the late night and afternoon of July 7 and 8. Thick line indicates surface elevation.

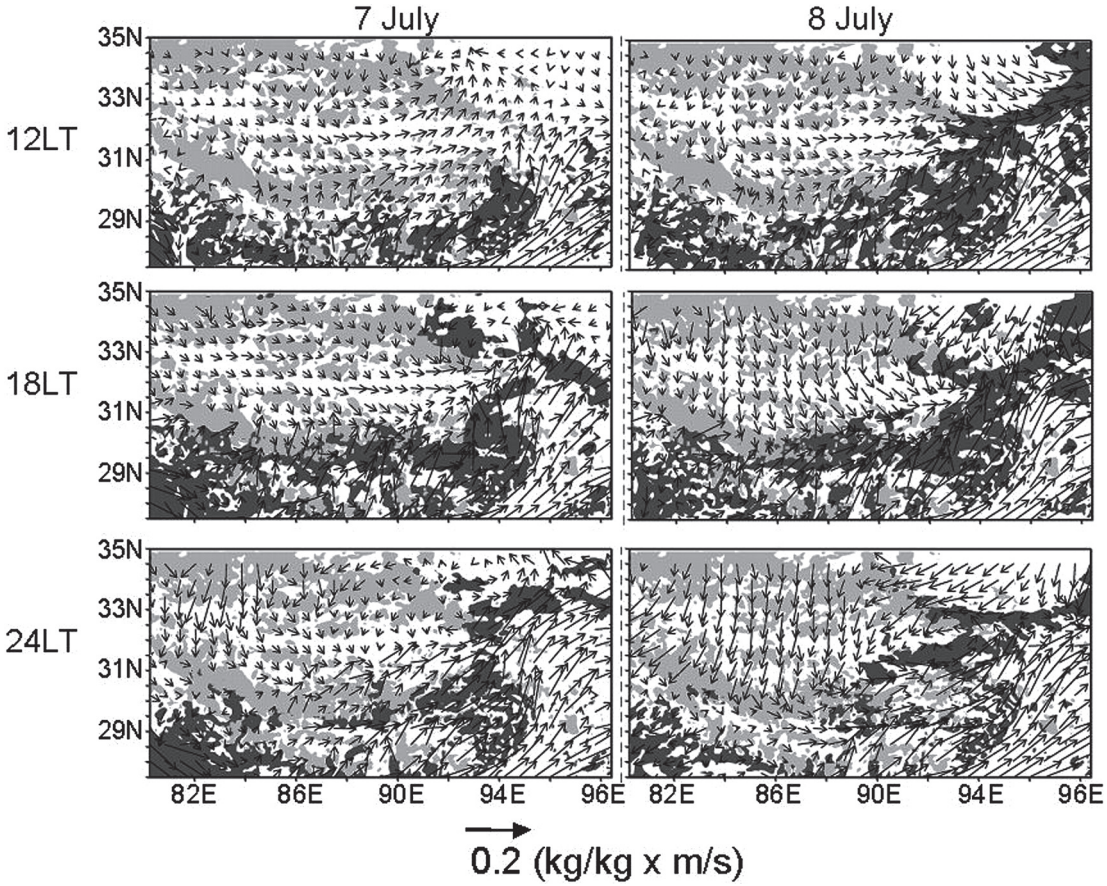


Fig. 8. Specific humidity (dark shade) and WV flux (vectors) at 5500 m a.s.l. simulated by NHM_6 on 7 July (left) and 8 July (right) in 1998. Dark shading corresponds to specific humidity of more than 0.008 kg/kg, and light shading shows mountain topography of more than 5000 m a.s.l.

## 4. Summary and discussion

Many past studies have focused on the thermodynamic function of the TP with large diurnal convective activities that are usually accompanied by strong land-atmosphere interactions under a prevailing Tibetan High. This study focused on the WV transport processes from the Indian Ocean into the TP under a prevailing of synoptic-scale trough during the 1998 monsoon season, when WV intrusion from outside was expected. The major results are summarized as follows.

1) According to the WV budget analysis, a large amount of WV intruded from the south and converged over the TP in the cases of the TR type. WV convergence associated with horizontal advection was scarce for the UH type.
2) A composite analysis of GAME reanalysis data showed large differences in the subcontinental scale WV flow pattern between the UH and TR, corresponding with the active/break phase of Indian monsoon activity. In the case of the UH type, a moist air mass passing over the BoB in the lower layer reached to the south of the Himalayas. WV was then transported westward before reaching over the TP due to a cyclonic circulation formed over the Indian subcontinent in the mid-troposphere. On the other hand, in the case of the TR type, low-level monsoon westerlies were directed to the foot of the Himalayas passing over central and northern India that provided WV intrusion into the TP.
3) A diurnal variation in WV advection from south of the Himalayas to the southeastern TP was identified by the NHM in a representative case of the TR type. The WV transport was complexly intertwined with some physical factors in the lower and middle troposphere. Then, Sche-

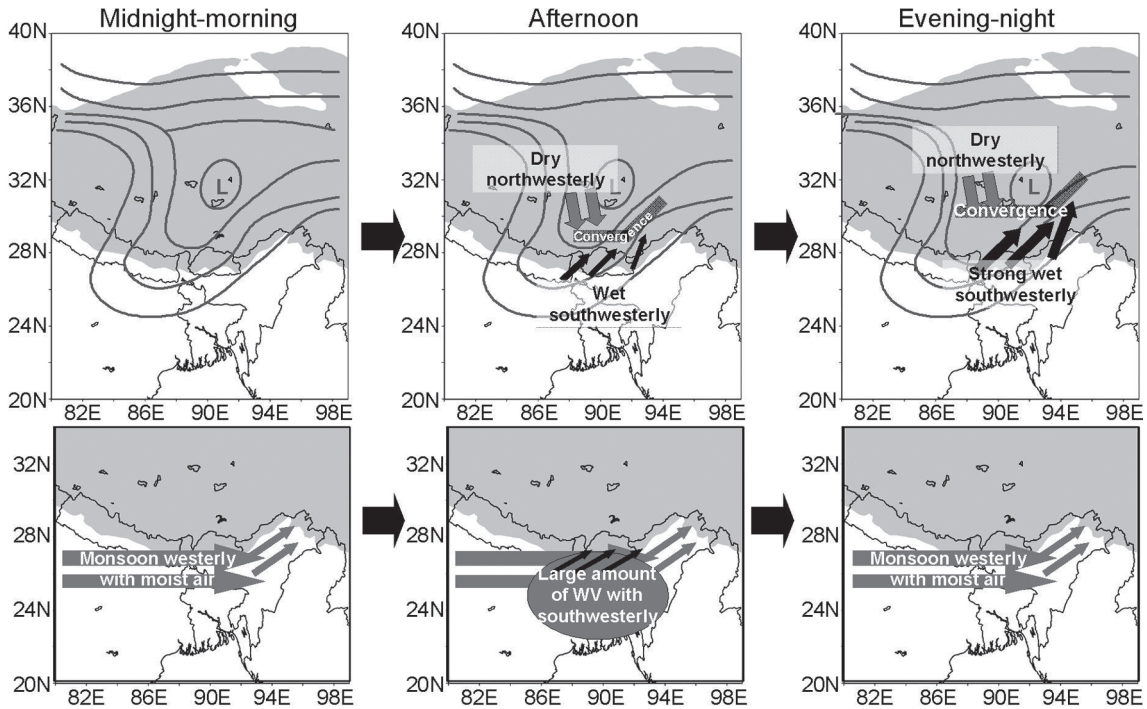


Fig. 9. Schematic diagrams of WV transport processes from south of the Himalayas to the TP in the TR case. Upper panels indicate the middle troposphere, and lower panels indicate the lower troposphere. Areas higher than 1500 m a.s.l. are shaded.

matic diagrams of the transport processes are shown in Fig. 9. WV supplied to the south of the Himalayas by monsoon westerlies in the lower troposphere reached 1500–2000 m a.s.l with the development of a mixing layer in the afternoon. At the same time, upslope wind in the southern slopes of the Himalayas lifted the moist air mass to the plateau level. Over the TP, a convergence zone of WV was formed by moist southwesterlies in front of the synoptic trough and a dry northwesterly behind it. This convergence zone expanded northward in the evening and disappeared by the next morning due to the weakening of a moist southwesterly crossing over the Himalayas. The results of the NHM simulation study suggest that WV transportation processes are composed by multiple steps.

In the NHM, WV distribution was limited in the south-southeastern TP, and did not expand to the north-northwestern areas. The prevailing TR type may strongly contribute to making the contrasts of the ground-surface condition, such as soil moisture and vegetation, between the northwestern and southeastern TP via a precipitation process. Further understanding of the structure of the mesoscale precipitation system associated with WV conversion in the southeastern TP is anticipated.

The timing of the passing of a synoptic trough was accompanied by the break phase of the Indian monsoon causing increase of precipitation in south of the Himalayas. It is well known that precipitation in the Himalayas is mostly provided in the night as introduced in the Section 1. Then, there must be a strong linkage between enhancement of the nighttime precipitation and prevailing of the WV transport into the TP in the case of the TR type.

Based on the NHM simulation study, the pumping up of WV to the same altitude of the plateau surface was attributed to a strong daytime upslope wind. However, the spatial resolution and calculating techniques are insufficient to simulate the detailed structure of the local circulation along with real topography of the Himalayas. In addition, few in-situ observatories are available from which to verify the simulation results. Improvements of simulation technique for WV circulation over the steep slopes and their verification by establishing observation network are required for further studies.

## Acknowledgements

We are grateful to the Meteorological Research Institute and Japan Meteorological Agency for permission to use the NHM numerical model. The GTOPO 30 data was provided by United States Geological Survey. The METEOSAT-5 image was provided by EUMETSAT. We would like to thank the National Institute for Environmental Studies and the Computer Centers at Tohoku University for using supercomputer. We are also grateful to the anonymous reviewers for helpful comments. Part of this study was supported by the Core Research for Evolutional Science and Technology of the Japan Science and Technology Agency.

## References

Barros, A.P., M. Joshi, J. Putkonen, and D.W. Burbank, 2000: A study of the 1999 monsoon rainfall in a mountainous region in central Nepal using TRMM products and rain gauge observations. *Geophys. Res. Lett.*, **27**, 3683–3686.

Barros, A.P. and T.J. Lang, 2003: Monitoring the monsoon in the Himalayas: observations in central Nepal, June 2001. *Mon. Wea. Rev.*, **131**, 1408–1427.

Bollasina, M., L. Bertolani, and G. Taritari, 2002: Meteorological observations at high altitude in the Khumbu valley, Nepal Himalayas, 1994–1999. *Bulletin of Glacier Research*, **19**, 1–11.

Chang, C.C., 1981: A contrasting study of the rainfall anomalies between central Tibet and central India during the summer monsoon season of 1979. *Bull. Amer. Meteo. Soc.*, **62**, 20–22.

Fujinami, H. and T. Yasunari, 2001: The seasonal and intraseasonal variability of diurnal cloud activity over the Tibetan Plateau. *J. Meteor. Soc. Japan*, **79**, 1207–1227.

Fujinami, H. and T. Yasunari, 2004: Submonthly variability of convection and circulation over and around the Tibetan Plateau during the boreal summer. *J. Meteor. Soc. Japan*, **82**, 1545–1564.

Goswami, B.N. and R.S. Ajaya Mohan, 2001: Intraseasonal oscillations and interannual variability of the Indian summer monsoon. *J. Climate*, **14**, 1180–1198.

Hahn, G.D. and S. Manabe, 1975: The role of mountains in the south Asian monsoon circulation. *J. Atmos. Sci.*, **32**, 1515–1541.

Ikawa, M., 1988: Comparison of some schemes for nonhydrostatic models eith orography. *J. Meteor. Soc. Japan*, **66**, 753–776.

Ikawa, M. and K. Saito, 1991: Description of a nonhydrostatic model developed at the Forecast Research Department of MRI. *Tech Rep. MRI*, **28**, 238 pp.

Inoue, J., 1976: Climate of Khumbu Himal. *Seppyo*, **38** (special issue), 66–73.

Kain, J.S. and J.M. Fritsch, 1990: A one-dimensional entraining/detraining plume model and its application in convective parameterization. *J. Atmos. Sci.*, **47**, 2784–2802.

Keshavamurty, R.N. and S.T. Awade, 1970: On the maintenance of the mean monsoon trough over north India. *Mon. Wea. Rev.*, **98**, 315–320.

Krishnamurti, T.N. and H.N. Bhalme, 1976: Oscillations of a monsoon system. Part I, observational aspects. *J. Atmos. Sci.*, **33**, 1937–1954.

Kurishnamurthy, V. and J. Shukla, 2000: Intraseasonal and interannual variability of rainfall over India. *J. Climate*, **13**, 4366–4377.

Kurita, N. and H. Yamada, 2008: The role of local moisture recycling evaluated using stable isotope data from over the middle of the Tibetan Plateau during the monsoon season. *J. Hydromet*, **9**, 760–775.

Kuwagata, T., A. Numagiti, and N. Endo, 2001: Diurnal variation of water vapor the central Tibetan Plateau during summer. *J. Meteor. Soc. Japan*, **79**, 401–418.

Lau, K.M. and P.H. Chan, 1986: Aspects of the 40–50 day oscillation during the northern summer as inferred from outgoing longwave radiation. *Mon. Wea. Rev.*, **114**, 1354–1367.

Li, C. and M. Yanai, 1996: The onset and interannual variability of the Asian summer monsoon in relation to land-sea thermal contrast. *J. Climate*, **9**, 358–375.

Mujumdar, V.R., U.V. Bhide, S.G. Nagar, S.P. Ghanekar, and P. Seetaramayya, 2005: Thermodynamic characteristics over north Bay of Bengal during active and weak monsoon phases of BOBMEX-1999. *J. Ind. Geophys. Union.*, **9**, 219–233.

Murakami, M., 1976: Analysis of summer monsoon fluctuations over India. *J. Meteor. Soc. Japan*, **54**, 15–31.

Murakami, M., 1977: Spectrum analysis relevant to Indian monsoon. *Pure Appl. Geophys.*, **115**, special issue, 1145–1166.

Murakami, T., 1986: *Active and break monsoon, Monsoon*. Tokyodo-syuppan, 108 pp. (in Japanese)

Numaguti, A., 1999: Origin and recycling process of precipitating water over the Eurasian continent: Experiments using an atmospheric general circulation model. *J. Geophys. Res.*, **104**, 1957–1972.

Ohata, T., K. Higuchi, and K. Ikegami, 1981: Mountain-valley wind system in the Khumbu Himal, east Nepal. *J. Meteor. Soc. Japan*, **59**, 753–762.

Ohsawa, T., H. Ueda, T. Hayashi, A. Watanabe, and J. Matsumoto, 2001: Diurnal variations of convective activity and rainfall in Tropical Asia. *J. Meteor. Soc. Japan*, **79**, 333–352.

Onogi, K., J. Tsutsui, H. Koide, M. Sakamoto, S. Kobayashi, H. Hatsushika, T. Matsumoto, N. Yamazaki, H. Kamahori, K. Takahashi, S. Kadokura, K. Wada, K. Kato, R. Oyama, T. Ose, N. Mannoji, and R. Taira, 2007: The JRA-25 Reanalysis. *J. Meteor. Soc. Japan*, **85**, 369–432.

Pant, S. P., 1983: A physical basis for changes in the phases of the summer monsoon over India. *Mon. Wea. Rev.*, 111, 487–495.

Rao, Y.P. and K.S. Ramamurthy, 1968: *Forecasting Manual Part I: Climatology of India and Neighborhood –2, Climate of India*, India Meteorological Department, Poona, India.

Sasaki, T., P. Wu, F. Kimura, T. Yoshikane, and J. Liu, 2003: Drastic evening increase in precipitable water vapor over the southeastern Tibetan Plateau. *J. Meteor. Soc. Japan*, **81**, 1273–1281.

Sato, T. and F. Kimura, 2005: Impact of diabatic heating over the Tibetan Plateauon subsidence over northeast Asian arid region. *Geophys. Res. Lett.*, **32**, L05809, doi:10.1029/2004GL022089.

Sato, T. and F. Kimura, 2007: How does the Tibetan Plateau affect the transition of Indian monsoon rainfall? *Mon. Wea. Rev.*, **135**, 2006–2015.

Takagi, T., F. Kimura, and S. Kono, 2000: Diurnal variation of GPS precipitable water at Lhasa in premonsoon and monsoon periods. *J. Meteor. Soc. Japan*, **78**, 175–180.

Tian, L., T. Yao, A. Numaguti, and W. Sun, 2001: Stable isotope variations in monsoon precipitation on the Tibetan Plateau. *J. Meteor. Soc. Japan*, **79**, 959–966.

Ueda, H. and T. Yasunari, 1998: Role of warming over the Tibetan Plateau in early onset of the summer monsoon over the Bay of Bengal and the South China Sea. *J. Meteor. Soc. Japan*, **76**, 1–12.

Ueno, K., 1998: Characteristics of Plateau-scale precipitation in Tibet estimated by satellite data during 1993 monsoon season. *J. Meteor. Soc. Japan*, **76**, 533–548.

Ueno, K., H. Fujii, H. Yamada, and L. Liu, 2001a: Weak and frequent monsoon precipitation over the TP. *J. Meteor. Soc. Japan*, **79**, 429–434.

Ueno, K., R.B. Kayastha, H.M.R. Chitrakar, O.R. Bajracharya, A.P. Pokhrel, H. Fujinami, T. Kadota, H. Iida, D.P. Manandhar, M. Hattori, T. Yasunari, and M. Nakawo, 2001b: Meteorological observations during 1994–2000 at the automatic weather station (GEN-AWS) in Khumbu region, Nepal Himalayas. *Bulletin of Glacier Research*, **18**, 23–30.

Ueno, K., K. Toyotsu, L. Bertolani, and G. Taritari, 2008: Stepwise onset of monsoon weather observed in the Nepal Himalayas. *Mon. Wea. Rev.*, **136**, 2507–2522.

Uppala, M.S., P.W. Kallberg, A.J. Simmons, U. Andrae, V. DA Costa Bechtold, M. Fiorino, J.K. Gibson, J. Haseler, A. Hernandez, G.A. Kelly, X. Li, K. Onogi, S. Saarinen, N. Sokka, R.P. Allan, E. Andersson, K. Arpe, M.A. Balmaseda, A.C.M. Beljaars, L. Vandeberg, J. Bidlot, N. Bormann, S. Caires, F. Chevallier, B.J. Hoskins, L. Isaksen, P.A.E.M. Janssen, R. Jenne, A.P. Mcnally, J.-F. Malfouf, K.E. Trenberth, A. Untch, D. Vasiljevic, P. Viterbo, and J. Woollen, 2005: The ERA-40 reanalysis. *Quart. J. Roy. Meteor. Soc.*, **131**, 2961–3012.

Uyeda, U., H. Yamada, J. Horikomi, R. Shirooka, S. Shimizu, L. Liping, K. Ueno, H. Fujii, and T. Koike, 2001: Characteristics of convective clouds observed by a Doppler radar at Naqu on Tibetan Plateau during the GAME-Tibet IOP. *J. Meteor. Soc. Japan*, **79**, 463–474.

Wu, G. and Y. Zhang, 1998: Tibetan Plateau forcing and the timing of the monsoon onset over South Asia and the South China Sea. *Mon. Wea. Rev.*, **126**, 913–927.

Yanai, M., C. Li, and Z. Song, 1992: Seasonal heating of the Tibetan Plateau and its effects on the evolution of the Asian summer monsoon. *J. Meteor. Soc. Japan*, **70**, 319–351.

Yanai, M. and C. Li, 1994: Mechanism of heating and the boundary layer over the Tibetan Plateau. *Mon. Wea. Rev.*, **122**, 305–323.

Yanai, M. and G. Wu, 2006: *Effects of the Tibetan Plateau, The Asian monsoon*, Praxis Pulishing Ltd.

Yamada, H. and H. Uyeda, 2006: Transition of the rainfall characteristics related to the moistening of the land surface over the central Tibetan Plateau during the summer of 1998. *Mon. Wea. Rev.*, **134**, 3230–3247.

Yamazaki, N., K. Takahashi, and A. Yatagai, 2003: *Report on the GAME Reanalysis. GAME Phase 1 Summary Repport.* (GAME Publ. No. 37), 81–87.

Yasunari, T., 1979: Cloudiness fluctuations associated with the northern hemisphere summer monsoon. *J. Meteor. Soc. Japan*, **57**, 227–242.

Yasunari, T., 1980: A quasi-stationary appearance of 30 to 40 day period in the cloudiness fluctuations during the summer monsoon over India. *J. Meteor. Soc. Japan*, **58**, 225–229.

Yasunari, T., 1981: Structure of an Indian summer monsoon system with around 40-day period. *J. Meteor. Soc. Japan*, **59**, 336–354.

Yasunari, T., 1998: Toward the implementation of the GAME-IOP 1998 –How is Asian monsoon forced by seasonal change of insolation?–. *Tenki*, **45**, 501–514. (in Japanese)

Ye, D. and G. Wu, 1998: The role of the heat source of the Tibetan Plateau in the general circulation. *Meteor. Atmos. Phys.*, **67**, 181–198.